Suppression of Aging in Mice by the Hormone Klotho

Hiroshi Kurosu,[1] Masaya Yamamoto,[1] Jeremy D. Clark,[1] Johanne V. Pastor,[1] Animesh Nandi,[1] Prem Gurnani,[1] Owen P. McGuinness,[3] Hirotaka Chikuda,[4] Masayuki Yamaguchi,[4] Hiroshi Kawaguchi,[4] Iichiro Shimomura,[5] Yoshiharu Takayama,[2] Joachim Herz,[2] C. Ronald Kahn,[6] Kevin P. Rosenblatt,[1] Makoto Kuro-o[1]*

A defect in *Klotho* gene expression in mice accelerates the degeneration of multiple age-sensitive traits. Here, we show that overexpression of *Klotho* in mice extends life span. Klotho protein functions as a circulating hormone that binds to a cell-surface receptor and represses intracellular signals of insulin and insulin-like growth factor 1 (IGF1), an evolutionarily conserved mechanism for extending life span. Alleviation of aging-like phenotypes in Klotho-deficient mice was observed by perturbing insulin and IGF1 signaling, suggesting that Klotho-mediated inhibition of insulin and IGF1 signaling contributes to its anti-aging properties. Klotho protein may function as an anti-aging hormone in mammals.

Klotho was originally identified as a mutated gene in a mouse strain that accelerates age-dependent loss of function in multiple age-sensitive traits (*1*). An insertional mutation that disrupts the 5′ promoter region of the *Klotho* gene resulted in a strong hypomorphic allele. Mice homozygous for the mutated allele ($KL^{-/-}$ mice) appeared normal until 3 to 4 weeks old but then began to manifest multiple age-related disorders observed in humans, including ectopic calcification, skin atrophy, muscle atrophy, osteoporosis, arteriosclerosis, and pulmonary emphysema. $KL^{-/-}$ mice suffered premature death around two months of age.

The *Klotho* gene encodes a single-pass transmembrane protein that is detectable in limited tissues, particularly the distal convoluted tubules in the kidney and the choroid plexus in the brain. Because a defect in the *Klotho* gene leads to systemic age-dependent

[1]Department of Pathology, [2]Department of Molecular Genetics, University of Texas (UT) Southwestern Medical Center at Dallas, 5323 Harry Hines Boulevard, Dallas, TX 75390–9072, USA. [3]Department of Molecular Physiology and Biophysics, Vanderbilt University School of Medicine, 702 Light Hall, Nashville, Tennessee 37232–0615, USA. [4]Department of Sensory and Motor System Medicine, University of Tokyo, 7-3-1 Hongo, Bunkyo, Tokyo 113-8655, Japan. [5]Department of Internal Medicine and Molecular Science, Graduate School of Medicine, Osaka University, 2-2 Yamadaoka, Suita, Osaka 565-0871, Japan. [6]Research Division, Joslin Diabetes Center, Department of Medicine, Harvard Medical School, One Joslin Place, Boston, MA 02215, USA.

*To whom correspondence should be addressed. E-mail: makoto.kuro-o@utsouthwestern.edu

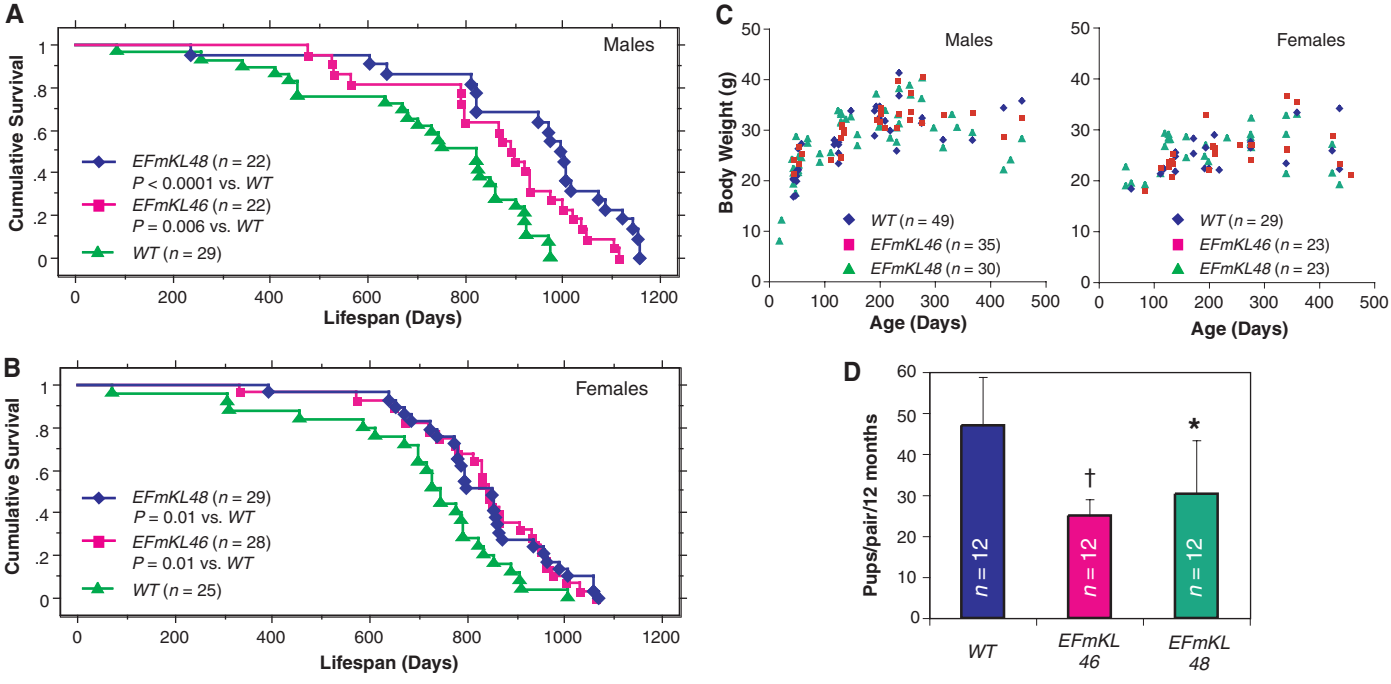

Fig. 1. Klotho overexpression extends life span in the mouse. Kaplan-Meier analysis of survival in (**A**) males [$P = 0.006$ in *EFmKL46* versus wild-type (WT) mice, and $P < 0.0001$ in *EFmKL48* versus wild type by log-rank test) and in (**B**) females ($P = 0.01$ in *EFmKL46* versus wild type, and $P = 0.01$ in *EFmKL48* versus wild type by log-rank test). The average life span of male wild-type, *EFmKL46*, and *EFmKL48* mice was 715 ± 44 days, 858 ± 40 days, and 936 ± 47 days (means ± SEM), respectively. The average life span of female wild-type, *EFmKL46*, and *EFmKL48* mice was 697 ± 45 days, 829 ± 32 days, and 830 ± 29 days, respectively. (**C**) Body weight of wild-type, *EFmKL46*, and *EFmKL48* mice. No significant difference in growth was observed. (**D**) Klotho overexpression reduces fecundity. Twelve breeding pairs at 12 weeks of age were set up for each genotype. The number of offspring generated during 12 months was recorded for each breeding pair. Although average litter size (pups per birth) of wild-type, *EFmKL46*, and *EFmKL48* pairs was not significantly different (6.6 ± 1.0, 6.1 ± 1.3, and 7.0 ± 1.2, respectively), the number of births (births per pair per 12 months) was fewer in transgenic mice pairs (7.2 ± 1.6, 4.2 ± 0.8, and 4.5 ± 2.2, respectively), resulting in significantly fewer offspring in transgenic pairs. Data are means ± SD. *, $P < 0.05$; †, $P < 0.01$ versus wild-type mice by analysis of variance (ANOVA).

degeneration, the Klotho protein may function through a circulating humoral factor that regulates the development of age-related disorders or natural aging processes (*2*). Notably, some single-nucleotide polymorphisms in the human *KLOTHO* gene are associated with altered life span (*3*) and altered risk for coronary artery disease (*4*), osteoporosis (*5*–*7*), and stroke (*8*).

Little is known about Klotho protein function and the molecular mechanism by which it suppresses the development of aging-like phenotypes. The extracellular domain of Klotho protein is composed of two internal repeats, KL1 and KL2, that share amino acid sequence homology to β-glucosidases of bacteria and plants (20 to 40% identity) (*1*). However, glucosidase activity is not present in recombinant Klotho protein (*9*), and the essential glutamate residue at the β-glucosidase active center is replaced with asparagine and alanine in KL1 and KL2, respectively (*10*). Here, we demonstrate that *Klotho* is an aging suppressor gene whose product functions as a hormone that inhibits intracellular insulin and IGF1 signaling.

Klotho overexpression extends life span in mice. We previously generated independent transgenic lines of mice that overexpress *Klotho* under the control of the human elongation factor 1α promoter (*1*) (*EFmKL46* and *EFmKL48*) (fig. S1). Here, we compared the life span of the transgenic mice with that of wild-type controls that are near-coisogenic by virtue of backcrossing onto the C3H background four times. Each line was previously confirmed to express functional Klotho protein from the transgene (*1*). Mice carrying the

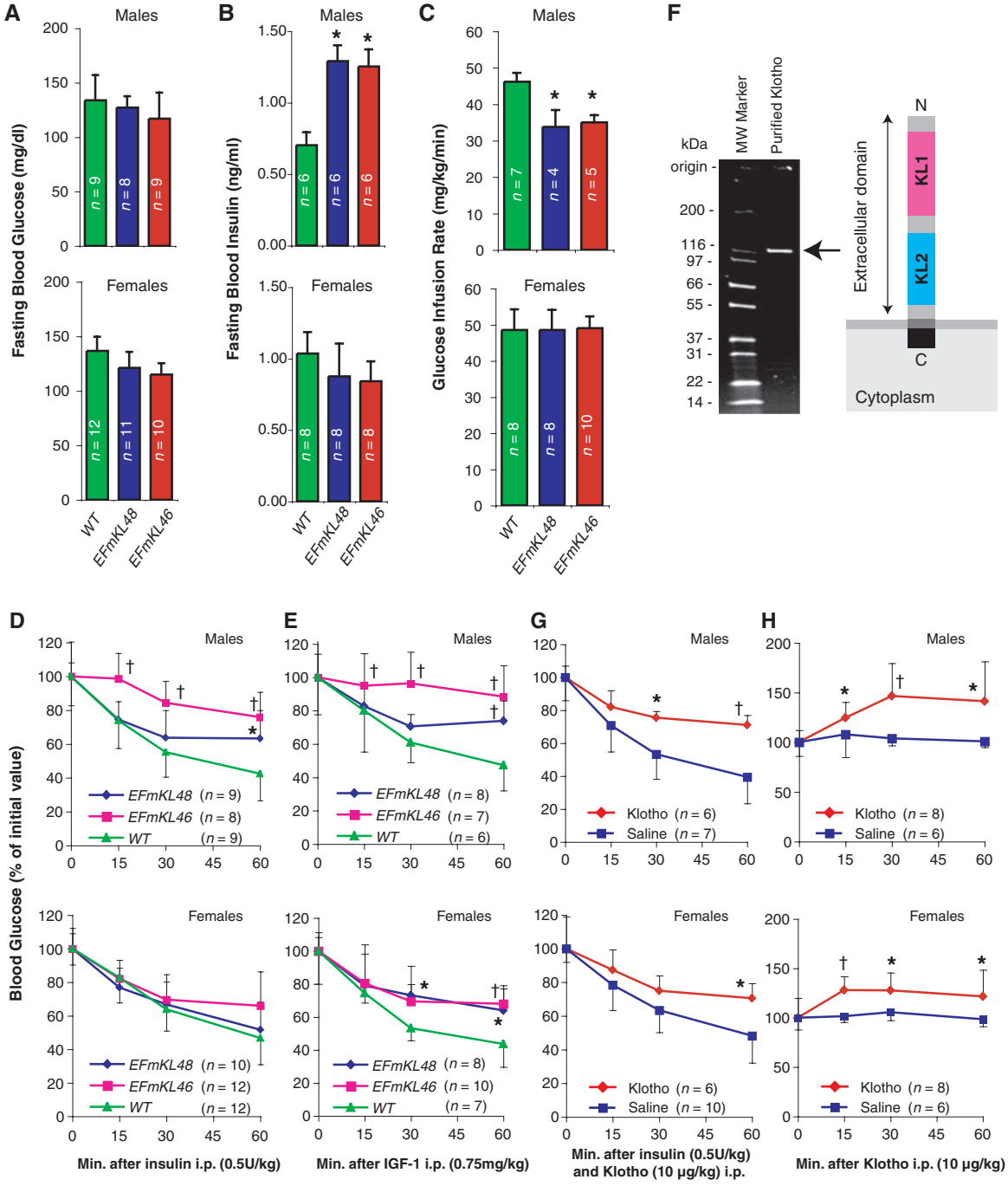

Fig. 2. Klotho increases resistance to insulin and IGF1. (**A** and **B**) Fasting blood glucose (A) and insulin (B) levels were compared between wild-type (WT), *EFmKL48*, and *EFmKL46* mice. (**C**) Hyperinsulinemic euglycemic clamp experiments. Glucose infusion rate (mg/kg/min) was compared between wild-type, *EFmKL48*, and *EFmKL46* mice. During the clamp experiments there were no differences in blood glucose concentration between wild-type, *EFmKL46*, and *EFmKL48* mice. The number of animals (*n*) for each group is indicated in the bars. (**D** and **E**) Insulin (D) and IGF1 (E) tolerance tests. Blood glucose levels after injection of insulin (0.5 U/kg) or IGF1 (0.75 mg/kg) were expressed as a percentage change from blood glucose concentration at time zero. Error bars indicate SD. *, $P < 0.05$ and †, $P < 0.01$ versus wild-type mice by ANOVA. (**F**) A schematic representation of Klotho extracellular peptide (right) and analysis of purified recombinant Klotho peptide by SDS-polyacrylamide gel electrophoresis (left). (**G**) The effect of Klotho injection on insulin tolerance in mice. Insulin tolerance tests were performed with age-matched wild-type mice immediately after intraperitoneal injection with saline or purified recombinant Klotho peptide (10 μg/kg). (**H**) The effect of Klotho injection on blood glucose levels. Saline or Klotho protein (10 μg/kg) was administered into age-matched wild-type mice by intraperitoneal injection. Error bars indicate SD. *, $P < 0.05$ and †, $P < 0.01$ versus saline-injected mice by ANOVA.

EFmKL46 or *EFmKL48* transgenic alleles, fed *ad libitum*, outlived wild-type controls by 20.0 and 30.8%, respectively, in males (Fig. 1A) and by 18.8 and 19.0%, respectively, in females (Fig. 1B).

Caloric restriction is associated with increased longevity in various species (*11*). To assess whether mice overexpressing Klotho were restricting their own diets, we monitored food intake and oxygen consumption in transgenic and wild-type mice for 24 hours at 32 to 36 weeks of age. No significant differences in these parameters were observed (table S1). Small body size is also associated with extended longevity in diet-restricted mice and in mice that are mutant for pituitary or growth hormone receptor function (*12*, *13*). However, we did not observe any substantial difference in growth between *EFmKL46*, *EFmKL48*, and wild-type mice (Fig. 1C). Both *EFmKL46* and *EFmKL48* breeding pairs generated fewer offspring than wild-type breeding pairs (Fig. 1D). As expected from the evolutionary theory of longevity, maximum fitness of the organism is a trade-off between life span and fertility (*14*). These data indicate that *Klotho* systemically modulates aging through mechanisms independent of food intake and growth, but potentially in association with reproduction.

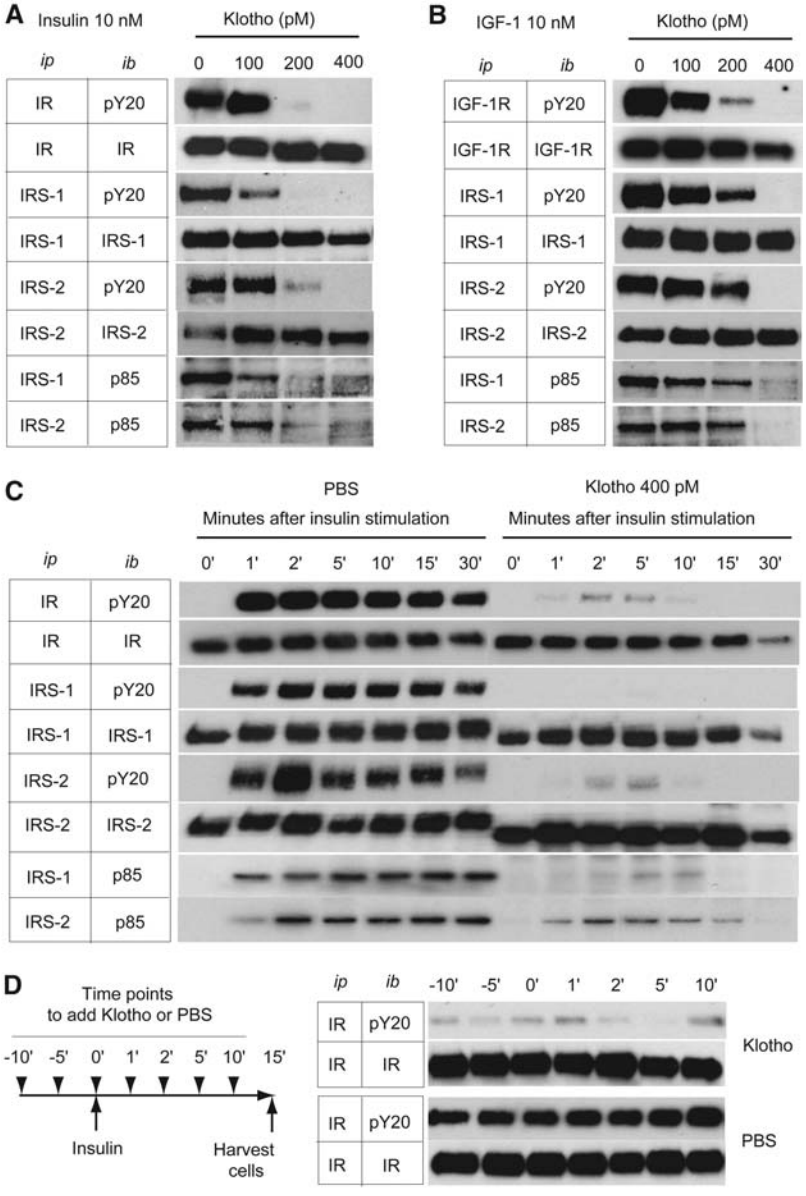

Fig. 3. Klotho protein inhibits intracellular insulin and IGF1 signaling. (**A** and **B**) Effect of Klotho on tyrosine phosphorylation of insulin and IGF1 receptors as well as IRS-1 and IRS-2, association of IRS-1 and IRS-2 with the PI3-kinase regulatory subunit (p85), and phosphorylation of Akt in L6 cells stimulated with 10 nM of insulin (A) or 10 nM of IGF1 (B). Antibodies used for immunoprecipitation (ip) and immunoblotting (ib) were indicated. IR, antibody to insulin receptor β chain; pY20, antibody to phosphotyrosine; IRS-1, antibody to IRS-1; IRS-2, antibody to IRS-2; p85, antibody to PI3-kinase regulatory subunit; IGF-1R, antibody to IGF1 receptor β chain. (**C**) A time course of the inhibitory effect of Klotho protein (400 pM) on insulin signaling in H4IIE cells. The cells were harvested before (0′) and at the indicated time points after insulin stimulation (10 nM). (**D**) Inactivation of activated insulin receptor by Klotho protein. H4IIE cells were stimulated with insulin (10 nM) at time 0′ and harvested 15 min later. Klotho (400 pM) or phosphate-buffered saline (PBS) was added at the indicated time points indicated (left panel). The cell lysates were immunoprecipitated with IR and immunoblotted with pY20 or IR (right panel).

Klotho increases resistance to insulin and IGF1. Many genetic data demonstrate that inhibited insulin and IGF1 signaling extends life span in animals from *C. elegans*, to *Drosophila*, to mice (*15*–*21*). Because Klotho must mediate aging through effects of a systemic hormone, we investigated whether the *Klotho* gene is involved in the inhibition of insulin or IGF1 signaling. Mice defective in *Klotho* gene expression have reduced blood glucose and insulin levels coupled with enhanced sensitivity to insulin (*22*).

We compared glucose metabolism in the Klotho-overexpressing transgenic mice with wild-type animals. Blood glucose levels were normal in each transgenic line (Fig. 2A). However, male *EFmKL46* and *EFmKL48* mice had higher blood insulin levels than did wild-type males (Fig. 2B), suggesting that the male transgenic mice are somewhat insulin resistant. We directly assessed sensitivity to insulin with a hyperinsulinemic euglycemic clamp (*23*). As expected, male *EFmKL46* and *EFmKL48* mice required lower glucose infusion rates than did wild-type males to maintain normal blood glucose levels (Fig. 2C). Furthermore, insulin and IGF1 tolerance tests revealed significant attenuation in hypoglycemic response to injected insulin and IGF1 in male transgenic mice (Fig. 2, D and E). Although we were unable to detect insulin resistance in female transgenic mice (Fig. 2, C and D), they were significantly resistant to IGF1 (Fig. 2E). These studies demonstrate that Klotho overexpression induces resistance to insulin and IGF1.

Klotho functions as a hormone. The extracellular domain of Klotho is shed on the cell surface and detected in the blood and cerebrospinal fluid in mice and humans (*24*). Immunoblot analysis of plasma with the use of rabbit anti-Klotho antiserum demonstrated that the extracellular Klotho peptide can be detected in wild-type, *EFmKL48*, and *EFmKL46* mice but not in $KL^{-/-}$ mice (fig. S2). Radioimmunoassay further demonstrated that Klotho peptide is ~100 pM in wild-type mice and about two times as high in the transgenic overexpression strains (fig. S3). The extracellular domain of Klotho may function as a hormone-like substance (*2*).

To assess the function of the Klotho extracellular peptide, we generated a soluble form of recombinant Klotho protein comprising the 952–amino acid extracellular domain, and de-

termined whether this promoted insulin resistance when injected into mice. Intraperitoneal injection of insulin (0.5 U/kg) and purified Klotho extracellular peptide (10 μg/kg, Fig. 2F) in wild-type male and female mice attenuated the hypoglycemic response expected from insulin alone (Fig. 2G). Klotho peptide alone rapidly increased blood glucose levels in male wild-type mice and to a smaller extent in females (Fig. 2H). However, Klotho peptide injection did not induce significant changes in blood insulin and glucagon levels (fig. S4), suggesting that Klotho peptide inhibits insulin action directly in peripheral tissues.

To test whether Klotho antagonizes insulin at receptive cells, we determined whether recombinant Klotho peptide would reduce glucose uptake by blocking insulin binding to the insulin receptor. We measured cellular glucose uptake in cultured myoblastic cells (L6) incubated with or without insulin in the presence or absence of 100 pM of Klotho extracellular peptide. Klotho peptide suppressed insulin-induced glucose uptake by 55% without reducing the binding of [^{125}I] insulin to the cells (fig. S5). Thus, Klotho does not appear to inhibit ligand-binding to the insulin receptor, suggesting that Klotho may block insulin action by disrupting one or more alternative insulin-dependent intracellular signaling pathways. Accordingly, we measured the potential for [^{125}I]-labeled Klotho to bind directly to the cell surface. Hepatoma cells bound [^{125}I] Klotho in a dose-dependent manner and saturated when the total Klotho concentration exceeded 600 pM, and unlabeled Klotho peptide inhibited the binding of [^{125}I] Klotho (fig. S6). Together, these observations suggest that cells present a receptor at their surface other than the insulin receptor that binds to the Klotho peptide.

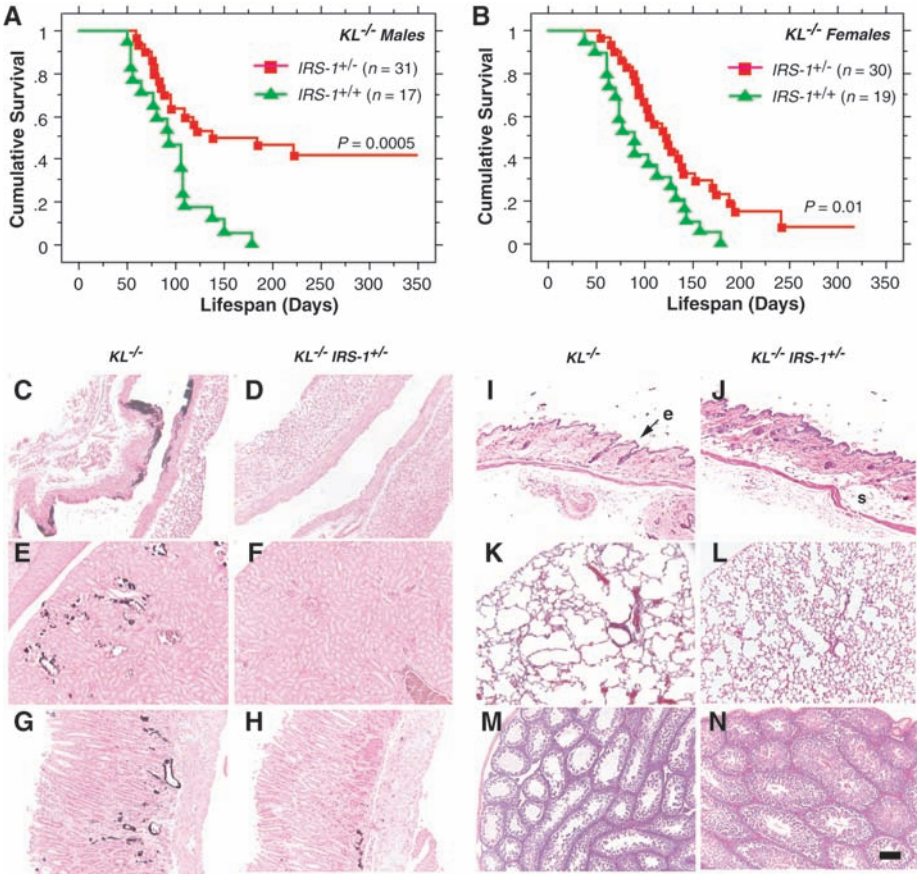

Fig. 4. Rescue of aging-like phenotypes in $KL^{-/-}$ mice by genetic intervention in insulin and IGF1 signaling. (**A** and **B**) Life-span extension in $KL^{-/-}$ mice by reducing IRS-1 expression. $KL^{-/-}$ mice heterozygous for an IRS-1 null allele ($IRS\text{-}1^{+/-}$) lived longer than those without the mutation ($IRS\text{-}1^{+/+}$) both in males ($P = 0.0005$ by log-rank test) and females ($P = 0.01$ by log-rank test). [(C) to (N)] Rescue of aging-like phenotypes in $KL^{-/-}$ $IRS\text{-}1^{+/-}$ mice at the histological level. Typical findings from four 8-week-old males of each genotype are shown. (**C** and **D**) Aorta (von Kossa staining). Calcification of arterial walls [black deposits in (C)] was decreased in $KL^{-/-}$ $IRS\text{-}1^{+/-}$ mice (D). (**E** and **F**) Kidney (von Kossa staining). Calcification of small arteries and renal tubules [black deposits in (E)] was decreased in $KL^{-/-}$ $IRS\text{-}1^{+/-}$ mice (F). (**G** and **H**) Stomach (von Kossa staining). Ectopic calcification in gastric mucosa and small arteries [black deposits in (G)] was alleviated in $KL^{-/-}$ $IRS\text{-}1^{+/-}$ mice (H). (**I** and **J**) Cross-sections of the skin. Hematoxylin-eosin (HE) staining. Reduction in epidermal layer (e) thickness observed in $KL^{-/-}$ mice (I) was improved and subcutaneous fat (s) was restored in $KL^{-/-}$ $IRS\text{-}1^{+/-}$ mice (J). (**K** and **L**) Lung (HE staining). Emphysematous changes, including enlargement of air spaces and destruction of the normal alveolar architecture were observed in $KL^{-/-}$ mice (K), but were alleviated in $KL^{-/-}$ $IRS\text{-}1^{+/-}$ mice (L). (**M** and **N**) Testis (HE staining). Seminiferous tubules were atrophic and no mature sperm was observed in $KL^{-/-}$ mice (M). Spermatogenesis was restored in $KL^{-/-}$ $IRS\text{-}1^{+/-}$ mice (N). All panels were shown in the identical magnification (×200). Scale bar, 200 μm.

Klotho inhibits intracellular insulin and IGF1 signaling. Because membrane-bound Klotho peptide must inhibit ligand activation of the insulin receptor within the cells, we investigated the influence of Klotho on insulin receptor signal transduction (*25*, *26*). We incubated L6 cells or rat hepatoma cells (H4IIE) with recombinant Klotho peptide and insulin (10 nM) or IGF1 (10 nM). Klotho peptide did not inhibit the binding of [^{125}I] insulin or [^{125}I] IGF1 (fig. S5) but suppressed ligand-stimulated autophosphorylation of insulin and IGF1 receptors in a dose-dependent manner (Fig. 3, A and B). Additionally, Klotho reduced activation of signaling events downstream of receptor activation, including tyrosine-phosphorylated insulin receptor substrate (IRS) 1 and 2, the association of the subunit of phosphoinositide 3–kinase p85 with IRS proteins (Fig. 3, A and B). Because the inhibitory effect of Klotho on insulin signaling was observed as early as 1 min after insulin stimulation (Fig. 3C), the decline in tyrosine-phosphorylated insulin and IGF1 receptors is unlikely due simply to the loss of receptors. Notably, Klotho peptide can inactivate active insulin receptors that were previously tyrosine phosphorylated by insulin stimulation. In H4IIE cells that were exposed to 10 nM insulin before adding Klotho peptide, Klotho suppressed tyrosine phosphorylation of the insulin receptor (Fig. 3D). We observed a similar effect on IGF1 receptor autophosphorylation in L6 cells with IGF1 before adding Klotho peptide (*9*). Importantly, the inhibitory effect of Klotho on autophosphorylation of receptor tyrosine kinases is specific. We observed no inhibitory effect of Klotho on the epidermal growth factor receptor and the platelet-derived growth factor receptor (fig. S7). Overall, Klotho appears to inhibit activation of the insulin and IGF1 receptor and to repress activated insulin and IGF1 receptors. Whether Klotho peptide functions by accelerating removal of tyrosine phosphorylation from the activated insulin receptor remains to be determined.

Inhibition of insulin and IGF1 signaling rescues $KL^{-/-}$ phenotypes. If the ability of Klotho to inhibit insulin and IGF1 signaling extends survival by retarding senescence, independent manipulations to inhibit insulin and IGF1 signaling may ameliorate some of the aging-like phenotypes in $KL^{-/-}$ mice. Accordingly, we crossed a loss-of-function mutation of IRS-1 into the $KL^{-/-}$ mice (*27*). Survival was improved in $KL^{-/-}$ mice heterozygous for an IRS-1 null allele ($KL^{-/-}$ $IRS\text{-}1^{+/-}$) relative to $KL^{-/-}$ control mice

(Fig. 4, A and B). In addition, $KL^{-/-}$ $IRS\text{-}1^{+/-}$ mice ameliorated many age-related pathologies typical of $KL^{-/-}$ mice, including arteriosclerosis, ectopic calcification, skin atrophy, pulmonary emphysema, and hypogonadism (Fig. 4, C to N). Heterozygosity of IRS-1 alone ($KL^{+/+}$ $IRS\text{-}1^{+/-}$ littermates) appears to have no effect on survival and the age-progressive degeneration when compared with those factors in wild-type littermates during these experiments (*9*).

Conclusion. We previously reported that a defect in *Klotho* gene expression leads to a syndrome that may resemble premature aging (*1*). Here, we show that overexpression of *Klotho* can extend life span, and we suggest that *Klotho* functions as an aging suppressor gene in mammals. We found that the extracellular domain of Klotho protein circulates in the blood and binds to a putative cell-surface receptor. Klotho has marked effects on insulin physiology, apparently because it suppresses tyrosine phosphorylation of insulin and IGF1 receptors, which results in reduced activity of IRS proteins and their association with PI3-kinase, thereby inhibiting insulin and IGF1 signaling. Extended life span upon negative regulation of insulin and IGF1 signaling is an evolutionarily conserved mechanism to suppress aging (*28*). Klotho appears to be a peptide hormone to modulate such signaling and thereby mediate insulin metabolism and aging.

References and Notes

1. M. Kuro-o *et al.*, *Nature* **390**, 45 (1997).
2. Y. Takahashi, M. Kuro-o, F. Ishikawa, *Proc. Natl. Acad. Sci. U.S.A.* **97**, 12407 (2000).
3. D. E. Arking *et al.*, *Proc. Natl. Acad. Sci. U.S.A.* **99**, 856 (2002).
4. D. E. Arking *et al.*, *Am. J. Hum. Genet.* **72**, 1154 (2003).
5. N. Ogata *et al.*, *Bone* **31**, 37 (2002).
6. K. Kawano *et al.*, *J. Bone Miner. Res.* **17**, 1744 (2002).
7. Y. Yamada, F. Ando, N. Niino, H. Shimokata, *J. Mol. Med.* **83**, 50 (2005).
8. D. E. Arking, G. Atzmon, A. Arking, N. Barzilai, H. C. Dietz, *Circ. Res.* **96**, 412 (2005).
9. M. Kuro-o *et al.*, data not shown.
10. F. Grabnitz, M. Seiss, K. P. Rucknagel, W. L. Staudenbauer, *Eur. J. Biochem.* **200**, 301 (1991).
11. R. Weindruch, R. L. Walford, S. Fligiel, D. Guthrie, *J. Nutr.* **116**, 641 (1986).
12. H. M. Brown-Borg, K. E. Borg, C. J. Meliska, A. Bartke, *Nature* **384**, 33 (1996).
13. R. A. Miller, *Sci. Aging Knowledge Environ.* **2001**, vp6 (2001).
14. G. C. Williams, *Evol. Int. J. Org. Evol.* **11**, 398 (1957).
15. C. Kenyon, J. Chang, E. Gensch, A. Rudner, R. Tabtiang, *Nature* **366**, 461 (1993).
16. J. Z. Morris, H. A. Tissenbaum, G. Ruvkun, *Nature* **382**, 536 (1996).
17. M. Tatar *et al.*, *Science* **292**, 107 (2001).
18. D. J. Clancy *et al.*, *Science* **292**, 104 (2001).
19. M. Holzenberger *et al.*, *Nature* **421**, 182 (2003).
20. M. Bluher, B. B. Kahn, C. R. Kahn, *Science* **299**, 572 (2003).
21. C. Kenyon, *Cell* **120**, 449 (2005).
22. T. Utsugi *et al.*, *Metabolism* **49**, 1118 (2000).
23. A. E. Halseth, D. P. Bracy, D. H. Wasserman, *Am. J. Physiol.* **276**, E70 (1999).
24. A. Imura *et al.*, *FEBS Lett.* **565**, 143 (2004).
25. A. R. Saltiel, C. R. Kahn, *Nature* **414**, 799 (2001).
26. D. LeRoith, C. T. Roberts Jr., *Cancer Lett.* **195**, 127 (2003).
27. E. Araki *et al.*, *Nature* **372**, 186 (1994).
28. M. Tatar, A. Bartke, A. Antebi, *Science* **299**, 1346 (2003).

29. We thank D. H. Wasserman and Vanderbilt Mouse Metabolic Phenotyping Center for physiological analysis of the mice; R. L. Dobbins for hyperinsulinemic euglycemic clamp experiments; J. A. Richardson and Molecular Pathology Core Facility at UT Southwestern for histological analysis; D. W. Russell at UT Southwestern for Klotho receptor identification; R. Komuro and H. Kuriyama at UT Southwestern for insulin and IGF1 signaling analysis; Genentech for providing IGF1; H. Masuda, T. Suga, R. Nagai, A. T. Dang, R. Shamlou, P. Bezzera, T. Reed, C. Iucu, W. Lai for earlier contributions and supports to this study; and E. C. Friedberg, M. S. Brown, and K. A. Wharton Jr. at UT Southwestern for critical reading of the manuscript. This work was supported in part by grants from Endowed Scholar Program at UT Southwestern (M.K.), Pew Scholars Program in Biomedical Science (M.K.), Eisai Research Fund (M.K.), High-Impact/High-Risk Research Program at UT Southwestern (M.K.), and NIH (R01AG19712 to M.K. and R01AG25326 to M.K. and K.P.R.). J.H. is supported by the NIH, the Perot Family Foundation, and the Humboldt Foundation.

Supporting Online Material
www.sciencemag.org/cgi/content/full/1112766/DC1
Materials and Methods
Figs. S1 to S7
Table S1
References

25 March 2005; accepted 4 August 2005
Published online 25 August 2005;
10.1126/science.1112766
Include this information when citing this paper.

REPORTS

Bright X-ray Flares in Gamma-Ray Burst Afterglows

D. N. Burrows,[1]* P. Romano,[2] A. Falcone,[1] S. Kobayashi,[1,3] B. Zhang,[4] A. Moretti,[2] P. T. O'Brien,[5] M. R. Goad,[5] S. Campana,[2] K. L. Page,[5] L. Angelini,[6,7] S. Barthelmy,[6] A. P. Beardmore,[5] M. Capalbi,[8] G. Chincarini,[2,9] J. Cummings,[6] G. Cusumano,[10] D. Fox,[11] P. Giommi,[8] J. E. Hill,[1] J. A. Kennea,[1] H. Krimm,[6] V. Mangano,[10] F. Marshall,[6] P. Mészáros,[1] D. C. Morris,[1] J. A. Nousek,[1] J. P. Osborne,[5] C. Pagani,[1,2] M. Perri,[8] G. Tagliaferri,[2] A. A. Wells,[5] S. Woosley,[12] N. Gehrels[6]

Gamma-ray burst (GRB) afterglows have provided important clues to the nature of these massive explosive events, providing direct information on the nearby environment and indirect information on the central engine that powers the burst. We report the discovery of two bright x-ray flares in GRB afterglows, including a giant flare comparable in total energy to the burst itself, each peaking minutes after the burst. These strong, rapid x-ray flares imply that the central engines of the bursts have long periods of activity, with strong internal shocks continuing for hundreds of seconds after the gamma-ray emission has ended.

Gamma-ray bursts (GRBs) are the most powerful explosions since the Big Bang, with typical energies around 10^{51} ergs. Long GRBs (duration > 2 s) are thought to signal the creation of black holes by the collapse of massive stars (*1–4*). The detected signals from the resulting highly relativistic fireballs consist of prompt gamma-ray emission (from internal shocks in the fireball) lasting for several seconds to minutes, followed by afterglow emission (from external shocks as the fireball encounters surrounding material) covering a broad range of frequencies from radio through x-rays (*5–7*). Because of the time needed to accurately determine the GRB position, most afterglow

[1]Department of Astronomy and Astrophysics, 525 Davey Lab, Pennsylvania State University, University Park, PA 16802, USA. [2]Istituto Nazionale di Astrofisica (INAF)–Osservatorio Astronomico di Brera, Via Bianchi 46, 23807 Merate, Italy. [3]Center for Gravitational Wave Physics, 104 Davey Lab, Pennsylvania State University, University Park, PA 16802, USA. [4]Department of Physics, University of Nevada, Box 454002, Las Vegas, NV 89154–4002, USA. [5]Department of Physics and Astronomy, University of Leicester, University Road, Leicester LE1 7RH, UK. [6]NASA/Goddard Space Flight Center, Greenbelt, MD 20771, USA. [7]Department of Physics and Astronomy, Johns Hopkins University, 3400 North Charles Street, Baltimore, MD 21218, USA. [8]Agenzia Spaziale Italiana Science Data Center, Via Galileo Galilei, 00044 Frascati, Italy. [9]Dipartimento di Fisica, Università degli studi di Milano-Bicocca, Piazza delle Scienze 3, 20126 Milan, Italy. [10]INAF–Istituto di Astrofisica Spaziale e Fisica Cosmica Sezione di Palermo, Via Ugo La Malfa 153, 90146 Palermo, Italy. [11]Department of Astronomy, California Institute of Technology, MS 105-24, Pasadena, CA, 91125, USA. [12]Department of Astronomy and Astrophysics, University of California, Santa Cruz, CA 95064, USA.

*To whom correspondence should be addressed. E-mail: burrows@astro.psu.edu